Finite element modeling and experimental investigation of infiltration of sodium chloride solution into nonviable liver tissue

Rimantas Barauskas, Antanas Gulbinas[1], Giedrius Barauskas[2]
Department of System Analysis, Kaunas University of Technology,
[1]Institute for Biomedical Research, [2]Department of Surgery, Kaunas University of Medicine, Lithuania

***Key words**: radiofrequency ablation; computational modeling; hydraulic conductivity; experimental research.*

***Summary.** The aim of this study was to establish a mathematical model of the infiltration of sodium chloride solution into cadaveric liver tissue.*

Methods. The time law of the flow of the infiltrated fluid at every node of the finite element model was obtained in terms of Darcy's velocity, pressure, and volumetric saturation fraction. The model equations interpret the liver tissue as a porous medium taking into account the hydraulic conductivity, capacity, and absorption mechanisms. Capability of the cadaveric liver tissue to absorb the fluid is taken into account by means of the nonlinear relationship of hydraulic capacity and absorption coefficients against the volumetric saturation fraction. To explain certain inadequacies between the computational model and experiment, the idealized models of empty blood vessels in the vicinity of the injection probe have been used. The model has been implemented in computational environment COMSOL Multiphysics. Experimental procedures were performed to analyze fluid infiltration and to calculate volume of fluid, which might be injected into certain volume of nonviable liver tissue.

Results. The necessary physical constants of hydraulic conductivity, capacity, and absorption of liver tissue have been determined by comparing the simulation results against the experimental data. The congruence of the modeling results against the experiment may be regarded as satisfactory.

Conclusion. The established model analyses distribution of injected solution taking into account the hydraulic conductivity, capacity, and absorption mechanisms of liver tissue. The obtained results are of importance developing complex models of electro-thermal heating coupled with heat advection by means of infiltrated sodium chloride solution.

Introduction

Performing liver tissue radiofrequency ablation (RFA) with cool-tip needle in experimental as well as in clinical setting is accompanied by continuous injection of sodium chloride solution through the active part of the ablation probe in order to prevent carbonization of tissues, which may impede or even block the heat transfer into the tissue. The infiltrating flow of the saline makes significant influence on the overall heat transfer process taking place during RFA due to certain amount of heating energy transferred into the tissue by advection, which is the transport of heat in a vector field of solution flow velocities (1). Together with the thermal conductivity of tissues, the two heat transfer mechanisms complete the full physical view of thermal processes to be taken into account in the mathematical description of RFA *ex vivo* experiments. As a result, advection determines enlargement of the thermal ablation zone and simultaneously influences restrained character of the temperature peak values in the nearest vicinity to the electrode, as opposed to purely conductive heat exchange mechanism. The latter phenomena should also be regarded in order to obtain clear margins of an ablated zone and to reduce the possibility of local recurrence following thermal ablation procedure.

During *in vivo* RFA processes, in addition to the heat conductance and heat advection by the flow of infiltrated solution, the advection-governed heat transfer takes place due to heat transport by the blood flow in liver tissue. The latter heat transfer mechanism is very complex due to nonuniform blood velocity field in the tissue and due to the presence of a dense network of tubular structures with varying calibers, which may sewer considerable amount of heating energy when

Correspondence to G. Barauskas, Department of Surgery, Kaunas University of Medicine, Eivenių 2, 50009 Kaunas, Lithuania. E-mail: giedrius.barauskas@gmail.com

the RFA probe is located in the vicinity of them.

Most of the research works published up to now employ simplified approaches for taking into account heat losses in the thermal ablation zone due to advection. Chang and Nguyen (2, 3) have employed the perfusion coefficient for taking into account volumetric heat losses due to thermal power absorbed by the blood. Moreover, cadaveric liver tissue contains a net of empty blood vessels of various calibers, which serve as channels for sewing the liquid. Neither blood nor the sodium chloride solution flow velocities were employed in the equations explicitly. Proper evaluation of fluid infiltration might give better insight into processes of heat distribution and might facilitate better RFA planning and improvement of clinical results.

This study presents a further effort to evaluate the flow velocity field caused by infiltration of sodium chloride solution injected through the holes of the RFA probe. In addition, in this work the model containing wells able to drain away the fluid from the injection zone has been presented and investigated.

Material and methods

Mathematical equations

The infiltration of sodium chloride solution into the liver tissue during RFA process is described by using the hydraulic conductivity model based on Darcy's law (4). In axisymmetric formulation, the partial differential equation (PDE), which describes the infiltration process in each finite element V reads as*:*

$$\frac{\partial}{\partial r}\left(2\pi rk\frac{\partial p}{\partial r}\right)+\frac{\partial}{\partial z}\left(2\pi rk\frac{\partial p}{\partial z}\right)=2\pi rs_h p+2\pi rc_h\frac{\partial p}{\partial t},\quad \in V\ , \qquad [1]$$

where: p – pressure presented as hydraulic head, measured in terms of height of equivalent water column [m], $k=\frac{q_h}{grad(p)}$ – hydraulic conductivity coefficient of the tissue, $\left[\frac{m}{s}\right]$; q_h – flux density (Darcy's velocity or volumetric rate across unit surface), [m/s]; c_h – hydraulic capacity of the porous medium. It is equal to Darcy's velocity as the fluid fills in the pores at $\frac{\partial p}{\partial t}=1$, [1/m]; s_h – hydraulic absorption coefficient of the porous medium. It is equal to Darcy's velocity as the fluid fills in the pores at p=1, [1/(ms)]; r, z – radial and axial coordinates of axially symmetric problem.

Two types of boundary conditions can be imposed (Fig. 1):

– Cauchy boundary conditions defining the flux density at infusion eyeholes;

$$n_r 2\pi rk\frac{\partial p}{\partial r}+n_z 2\pi rk\frac{\partial p}{\partial z}=-2\pi rq_{h0},\quad \in S_q\ , \qquad [2]$$

– Dirichlet boundary conditions defining the prescribed pressure at the boundary of the investigated domain as;

$$p=0;\quad \in S_p\ . \qquad [3]$$

Nonlinear model of hydraulic capacity and absorption.

The saturation of the pores of dead liver tissue by fluid is measured in terms of dimensionless quantity:

$$\gamma(\tilde{t},r,z)=2\pi\int_0^{\tilde{t}}\left(s_h rp+c_h r\frac{\partial p}{\partial t}\right)dt, \qquad [4]$$

which determines the volumetric saturation fraction (VSF) of the liver tissue (here the volume of the tissue is assumed to include the volume of pores) at point (r, z) filled by the fluid during time interval $[0,\tilde{t}]$ because of hydraulic capacity and absorption properties of the tissue.

Let γ_0 be the maximum VSF of the tissue, which may be filled in by the fluid. We model the tissue saturation effect by assuming that coefficients c_h, s_h are nonlinear and depend on VSF γ as follows:

$$c_h=c_{h0}e^{-a\left(\frac{\gamma}{\gamma_0}\right)^b};\quad s_h=s_{h0}e^{-a\left(\frac{\gamma}{\gamma_0}\right)^b}. \qquad [5]$$

Two possible choices of coefficient values a and b give the relationships presented in Fig. 2.

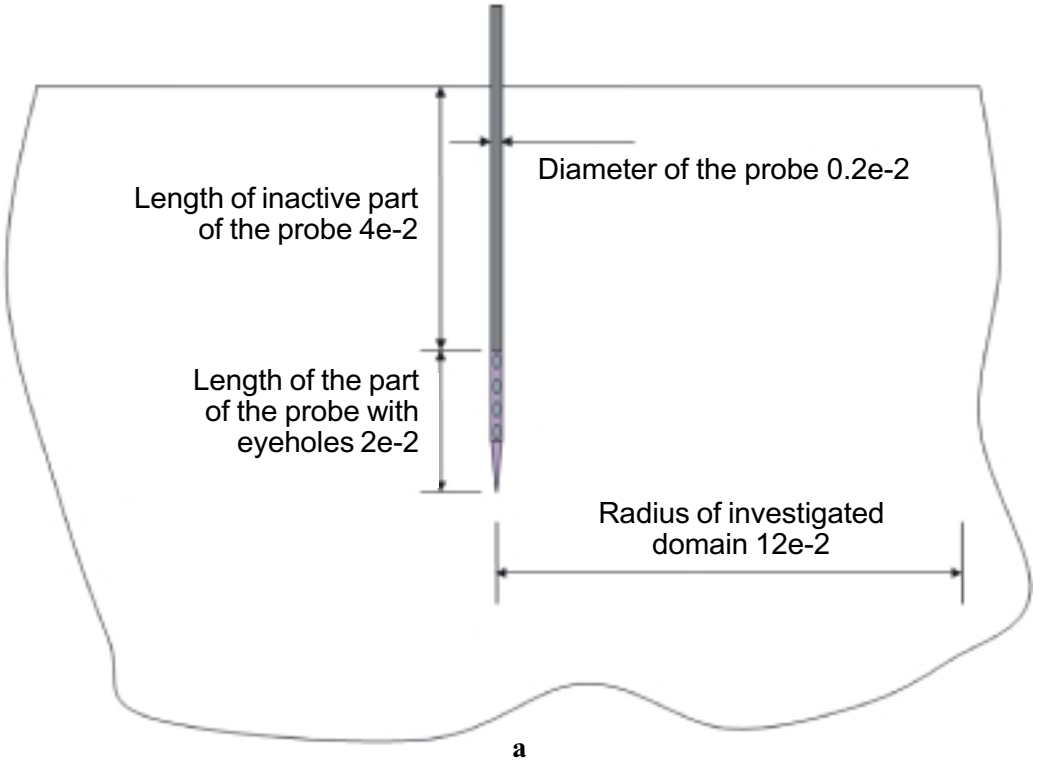

a

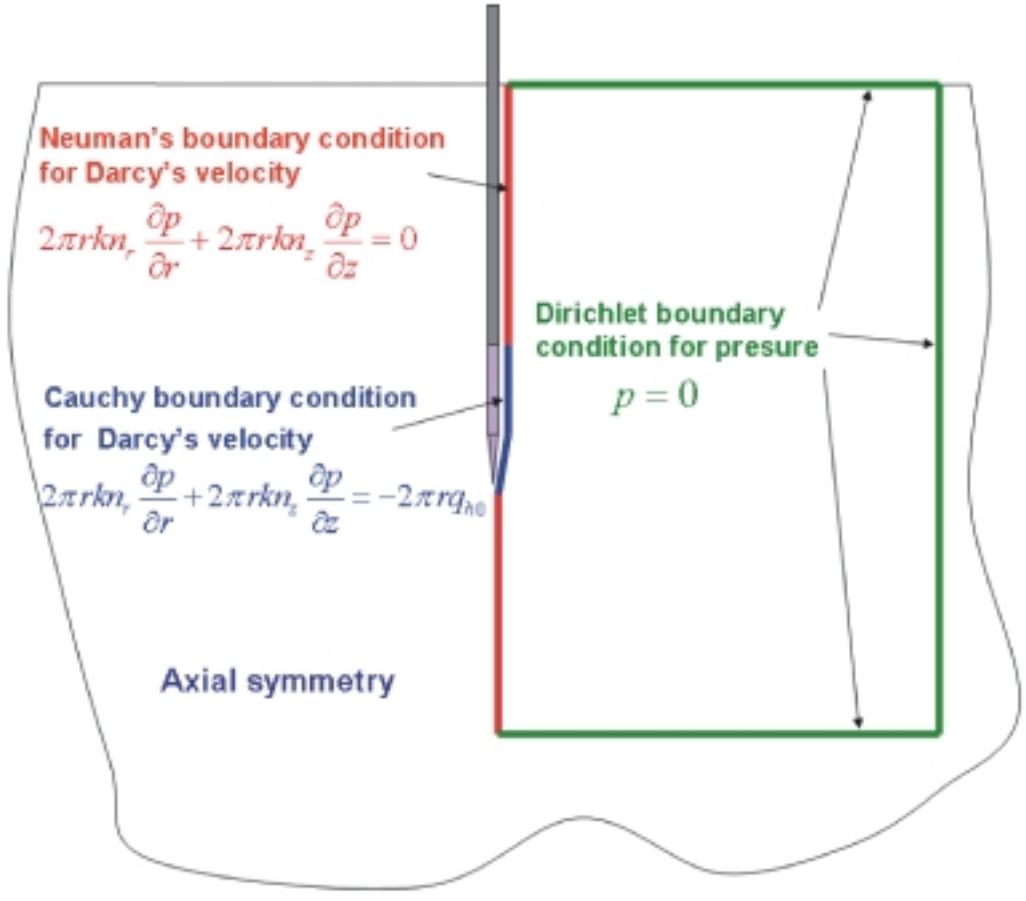

b

Fig. 1. **Scheme of the investigated domain**

a – geometry of investigated axisymmetric domain; b – boundary conditions.

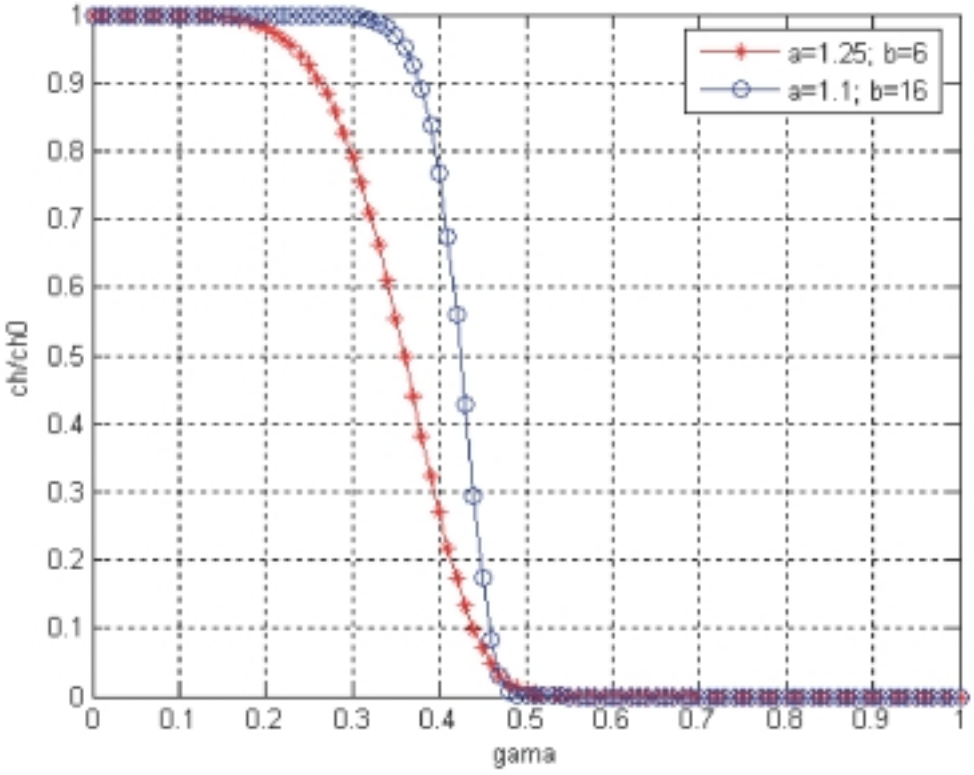

Fig. 2. **Dependency of relative hydraulic capacity coefficient on the volumetric fraction of tissue filled in by the fluid (saturation point γ_0=0.47)**

General form of equations in COMSOL Multiphysics computational environment

In COMSOL Multiphysics finite element analysis environment the partial differential equations [1] along with relation [4] with boundary conditions [2], [3] are presented in the "general" form as:

$$d_a \begin{Bmatrix} \dot{\gamma} \\ \dot{p} \end{Bmatrix} + \nabla \cdot \Gamma = F, \quad \in V \qquad [10]$$

with boundary conditions

$$\begin{cases} -\vec{\mathbf{n}} \cdot \Gamma = G; & \in S \\ 0 = R & \in S \end{cases}, \qquad [11]$$

where:

$$d_a = \begin{bmatrix} -1 & 2\pi r c_h \\ 0 & 2\pi r c_h \end{bmatrix}; \quad \Gamma = -\begin{Bmatrix} \begin{bmatrix} 0 \\ 0 \end{bmatrix} \\ \begin{bmatrix} 2\pi r k \dfrac{\partial p}{\partial r} \\ 2\pi r k \dfrac{\partial p}{\partial z} \end{bmatrix} \end{Bmatrix}; \quad F = \begin{Bmatrix} -2\pi r s_h p \\ -2\pi r s_h p \end{Bmatrix}; \quad \in \Omega \qquad [12]$$

$$G = \begin{bmatrix} 0 \\ q_{h0} \end{bmatrix}; \quad R = \begin{bmatrix} 0 \\ p - p_0 \end{bmatrix}, \qquad [13]$$

$$c_h = c_{h0} e^{-a\left(\frac{\gamma}{\gamma_0}\right)^b}; \quad s_h = s_{h0} e^{-a\left(\frac{\gamma}{\gamma_0}\right)^b}; \quad a = 1.25;\ b = 6;\ \ (a = 1.1;\ b = 16) \qquad [14]$$

q_{h0} – prescribed flux density at the part of the probe supplied with infusion eyeholes or q_{h0}=0 at the inactive zone of the probe.

The Dirichlet boundary condition

$$\begin{bmatrix} 0 \\ p - p_0 \end{bmatrix} = 0, \quad \in S_p \qquad [15]$$

is applied at distant edges of the investigated domain with p_0=0.

Experimental setup

Experimental model of fluid infiltration into nonviable tissue was designed utilizing cadaveric porcine liver (average weight 2300 g) and 0.9% sodium chloride solution, generally used in RFA procedures in clinical and experimental settings. Normal saline was colored by adding methylene blue to obtain well-marked trace of infiltrated liquid in cadaveric porcine liver. Infiltration procedure was performed at room temperature.

The 16-gauge RFA cooled-tip electrode needle with a 2-cm-exposed tip was used. After placement of the RFA needle in a randomly selected part of liver at a depth of 4 cm, infiltration was started. The solution was infused by means of automatic syringe at a constant speed of 90 mL/h for 10 min. The experiment was repeated five times in different cadaveric livers.

After termination of infusion with colored saline, the liver tissue was incised longitudinally along the needle and, afterwards, along the needle channel to disclose the central portion of the colored liver volume. The colored oval of liver tissue was then measured to obtain transverse half-width and longitudinal half-width of the infiltrated zone. Individual values were recorded accordingly. Average values were calculated as median and mean with standard deviation.

Experimental model to calculate peak volume of fluid, which might be injected into certain volume of nonviable tissue (volumetric saturation fraction, VSF), was designed utilizing cadaveric porcine liver and 0.9% sodium chloride solution at room temperature. Liver preparations at an average volume of 23.6±2.0 mL were excised out of cadaveric porcine liver (average weight 2300 g). Volume of excised liver tissue was measured by displacement of normal saline in calibrated flask (Archimedes principle).

The 16-gauge RFA cooled-tip electrode needle with a 2-cm-exposed tip was used. After placement of the RFA needle in the liver tissue preparation at a depth of 4 cm, infiltration was started. The solution was infused by means of automatic syringe at a constant speed of 90 mL/h for 30 min. The experiments were repeated five times with different cadaveric liver preparations. After termination of infusion, volume of infiltrated liver tissue preparation was measured by displacement of normal saline in the same calibrated flask. Individual values of liver preparation volume and infiltrated liver preparation volume were recorded. Volumetric saturation fraction, expressed as proportion of infiltrated fluid to liver preparation volume, was calculated accordingly.

Results

Experimental results

Experimental model of fluid infiltration in cadaveric porcine liver produced an oval-shaped zone saturated with methylene blue-colored saline (Fig. 3). Mean half-widths of longitudinal and transversal dimensions of ovals, produced in the experimental setting, were 3.5± 0.1 and 1.6±0.6, respectively. Detailed results of experiments on tissue infiltration are presented in Table 1.

Experimental model to calculate volume of fluid, which might be injected into certain volume of nonviable tissue, utilized liver preparation with a mean volume of 23.6 mL. The mean infiltrated fluid volume was 11.2 mL. Analysis of obtained results revealed that VSF varied among experiments from 0.454 to 0.500 with a mean value of 0.475 (Table 2).

Numerical results

The modeling results, such as the time law of the

Table 1. **Experimental data of cadaveric porcine liver tissue infiltration by methylene blue colored saline**

Measurement	Experiment No.					Mean±SD
	1	2	3	4	5	
Longitudinal half-width of the oval, cm	3.5	3.4	3.4	3.5	3.6	3.5±0.1
Transversal half-width of the oval, cm	1.1	2.3	1.4	1.2	2.2	1.6±0.6

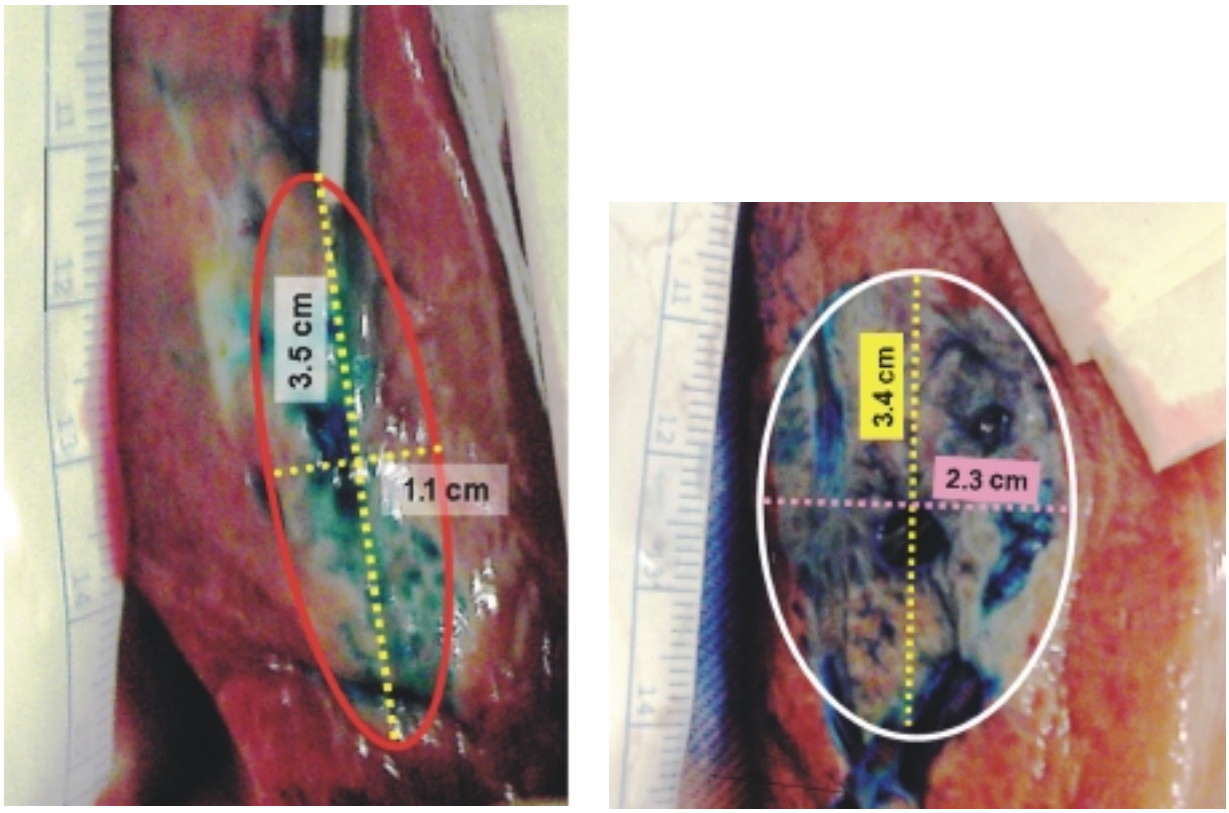

a **b** 5e7

Fig. 3. **Experimentally obtained zone of the liver tissue filled with the colored sodium chloride solution after 10 min of injection at a rate of 90 mL/h**

(a) and (b) correspond to experiments carried out at two different portions of the liver.

Table 2. **Volume of fluid injected into certain volume of nonviable liver tissue preparations in experimental setting with calculated volumetric saturation fraction (VSF)**

Measurement	Experiment No.					Mean±SD
	1	2	3	4	5	
Volume of excised tissue, mL	21	22	26	24	25	23.6±2.07
Volume of injected saline, mL	10	10	12	12	12	11.2±1.14
Volumetric saturation fraction	0.476	0.454	0.462	0.500	0.480	VSF=0.47

saturation fraction of pores in the tissue in the vicinity of the probe, the pressure in the tissue, as well as the velocity field of the injected fluid in terms of the Darcy's velocity are obtained at all nodes of the finite element mesh presented in Fig. 4. Along with contour plots, the graph relationships are presented along four selected lines (Fig. 5).

The tissue saturation model based on nonlinear dependences of hydraulic capacity and/or absorption coefficients based on relation [14] has been used. The coefficient values a=1.1; b=16 and experimentally measured maximum VSF of the cadaveric liver tissue as γ_0=0.47 were employed. The material parameters such as hydraulic conductivity coefficient k, hydraulic capacity coefficient c_h, and absorption coefficient s_h have been found by comparing the computed results against the experimental ones.

The model equations based on PDE [1] and the "forcing" term given in the form of boundary condition [2] imply that the value of integral [4] providing the VSF values at a point of the model is dependent only on the ratios $\frac{c_h}{k}$ and $\frac{s_h}{k}$. Fig. 6 presents the results of VSF distribution in the vicinity of the probe after

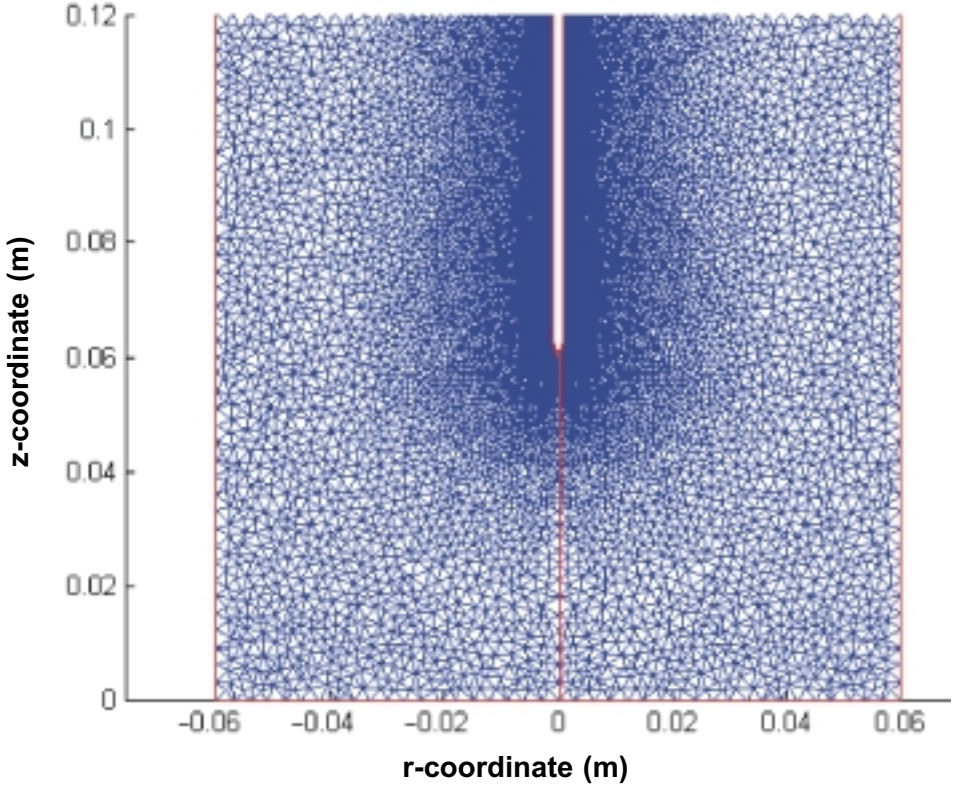

Fig. 4. **Finite element mesh containing 19 700 nodes, 38 640 elements**
Only the right-hand side represents the computational domain, the other side being geometrically reflected for visualization purposes.

10 min of injection of colored sodium chloride solution at an injection rate of 90 mL/h. Tissue saturation mechanism based purely on tissue hydraulic capacity has been assumed by taking $\frac{s_h}{k} = 0$. Different values of $\frac{c_h}{k}$ correspond to situations in which the hydraulic conductance (a) or hydraulic capacity (d) infiltration mechanism was prevailing as well as when both of them were significant simultaneously (b, c).

Fig. 7a presents the VSF values obtained in the model along line *linh2* (horizontal line in the middle of the active zone of the probe, directed outwards to the surface of the probe, see Fig. 5). Fig. 7b presents the VSF values obtained in the model along line *linh2* obtained by assuming hydraulic absorption mechanism rather than the hydraulic capacity, where the relative absorption coefficient is nonlinear *versus* the VSF value as presented in Fig. 2. In further calculations, we restrict ourselves with hydraulic capacity model by assuming s_h=0 everywhere. The choice is based on the fact that the hydraulic capacity model provides more strictly defined boundaries of the infiltrated zone, compare curves Fig. 7a and b where in case (a) the slope descends down practically to zero value, and is closer to reality observed in our experiments. As a checkpoint, the measurements of the oval form of the saturated tissue zone were compared in calculations and in the experiment.

In the model, the half-width of the ovals was determined by analyzing the curves in Fig. 6a. We assumed that the zone reached by the infiltrating fluid was where the VSF value $\gamma \geq 0.01$.

Values of equivalent hydraulic conductivity and/or absorption coefficients may be found, which enable to represent the overall injection and infiltration process satisfactorily. As an example, values $\frac{c_h}{k} = 1\times10^8$ and $\frac{c_h}{k} = 5\times10^7$ provide the computation results close to real measured situations presented in Fig. 3a and b, respectively, and may be used for modeling the infiltration processes in liver tissues.

Fig. 8 presents the values of the pressure in terms of $p\times k$ along reference lines *linv, linh1, linh2,* and *linh3* after 10 min of injection at a rate of 90 mL/h.

Discussion

The presented flow model is similar to that of Darcy's flow of the fluid through porous medium (4),

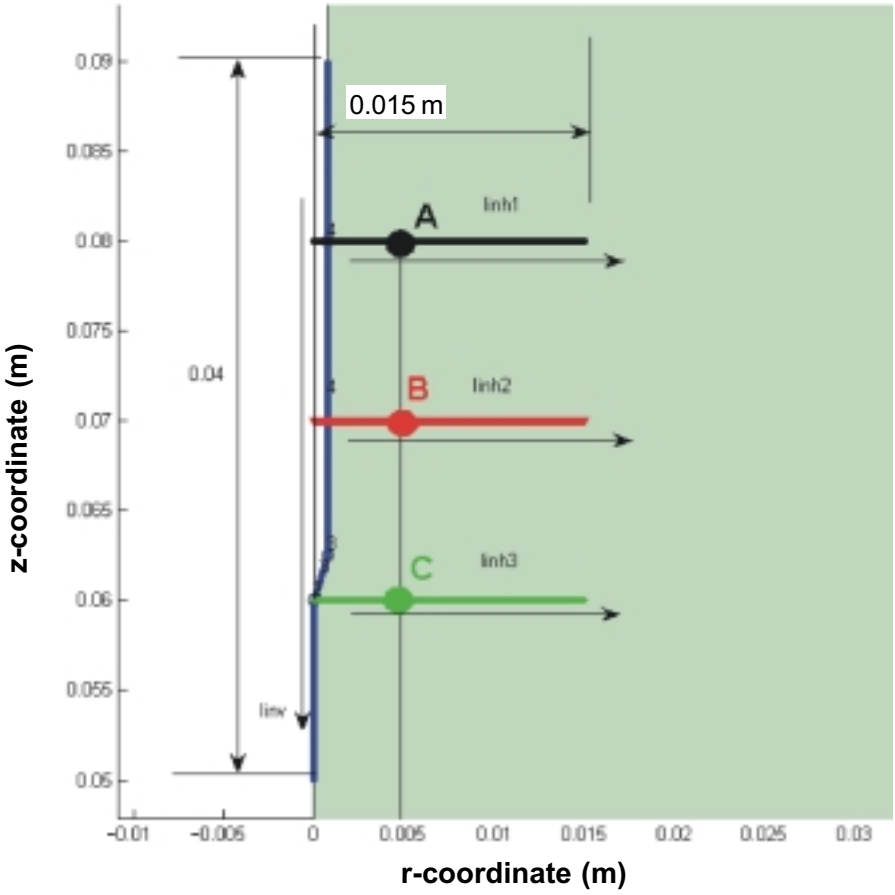

***Fig. 5.* Reference lines for plotting graph relationships**

linv – line along electrically active part of the probe; *linh1, linh2, linh3* – horizontal radial segments of the axisymmetric domain directed outwards from the surface of the probe.

which is assumed as governed by the hydraulic conductivity model and is widely used in many engineering applications. Hydraulic conductivity is a property of porous medium that describes the ease with which fluid can move through pore spaces. We assume that the role of the "pores" in the liver tissue is played by intercellular spaces and empty blood vessels of small caliber. Hydraulic conductivity is the proportionality constant in Darcy's law, which relates the amount of fluid, which will flow through a unit cross-sectional area of aquifer under a unit gradient of hydraulic head. It is analogous to the thermal conductivity of materials. It depends on the intrinsic permeability of the material and on the degree of saturation. The model is supplemented with the nonlinear hydraulic capacity term evaluating the possibility of a nonviable tissue to accommodate certain volume of a fluid within its intercellular space until the saturation point is reached. The amount of accommodated fluid volume is expressed in terms of VSF, defined by relation [4]. To our knowledge, no values of the hydraulic conductivity, capacity, and absorption coefficients of the liver tissue have been reported in the literature so far. The presented model of the sodium chloride infiltration process is a simplification of the real process in the sense that it assumes the liver tissue as a homogeneous porous material. In reality, nonviable liver tissue contains a lot of empty blood vessels of various calibers, which serve as channels for sewing the liquid. Actually, their influence can be approximately evaluated by assuming equivalent hydraulic conductivity and capacity coefficients integrally representing the behavior of the real tissue.

We investigated the infiltration process of fluid into the tissue following injection of normal saline through the eyeholes of the active part of the probe. The results provided by pure hydraulic capacity and hydraulic absorption models enable to conclude that there are no essential differences between the two models when the full saturation effect is taken into account by means of nonlinearly varying coefficients, c_h and s_h.

The analysis indicated that the liver tissue contains a dense net of blood vessels, and therefore in reality is not a homogeneous porous medium. The blood vessels

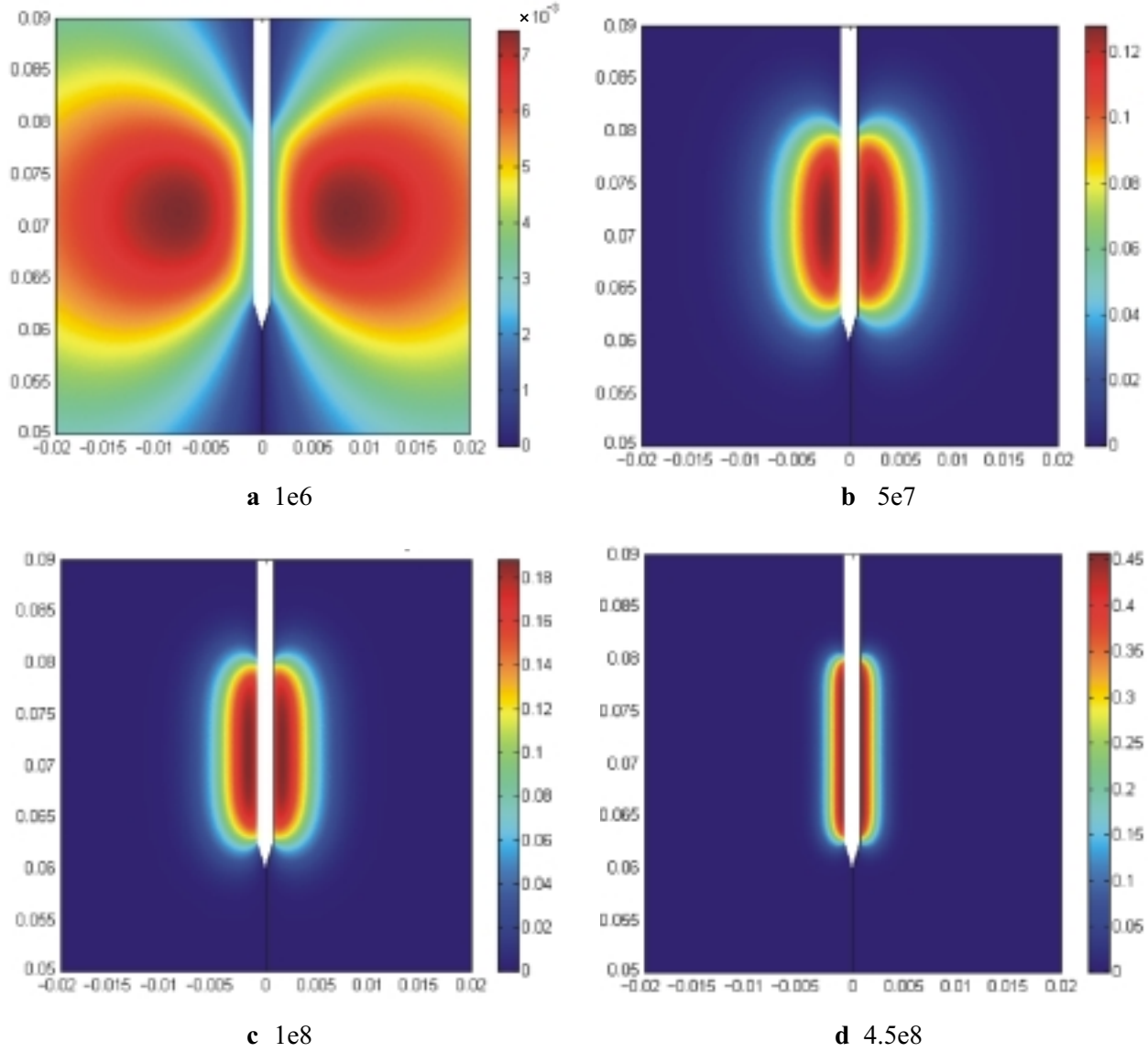

Fig. 6. **Distribution of volumetric saturation factor in the vicinity of the probe after 10 min of injection of colored sodium chloride solution at an injection rate of 90 mL/h and $\frac{S_h}{k}$=0:**

a – $\frac{c_h}{k}=10^6$; *b* – $\frac{c_h}{k}=5\times10^7$; *c* – $\frac{c_h}{k}=1\times10^8$; *d* – $\frac{c_h}{k}=4.5\times10^8$.

are empty in the cadaveric liver and serve as natural "wells" able to absorb certain amounts of the injected sodium chloride solution. The Darcy's flow with saturation model can serve only as the first and quite rough approximation of the real infiltration process in the liver tissue. Nevertheless, values of equivalent hydraulic conductivity and/or absorption coefficients may be found, which enable to represent the overall injection and infiltration process satisfactorily.

An alternative approach to the tissue saturation model is to evaluate the influence of empty blood vessels explicitly by presenting them as empty wells in the tissue able to accept the fluid. Mathematically the boundary condition at well edges is assumed as zero-pressure (*p=0*), Fig. 9. In axisymmetric formulation, the presented "blood vessels" are rather hypothetical, as each of them is modeled as an empty torus. In full volumetric presentation, real geometry of blood vessels could be presented; however, difficulties may appear because of complexity and varying density of tubular net in liver tissue.

A non-guided placement of the RFA needle may possibly result in drainage of the injected fluid to some vascular structures. In clinical settings, RFA is mainly

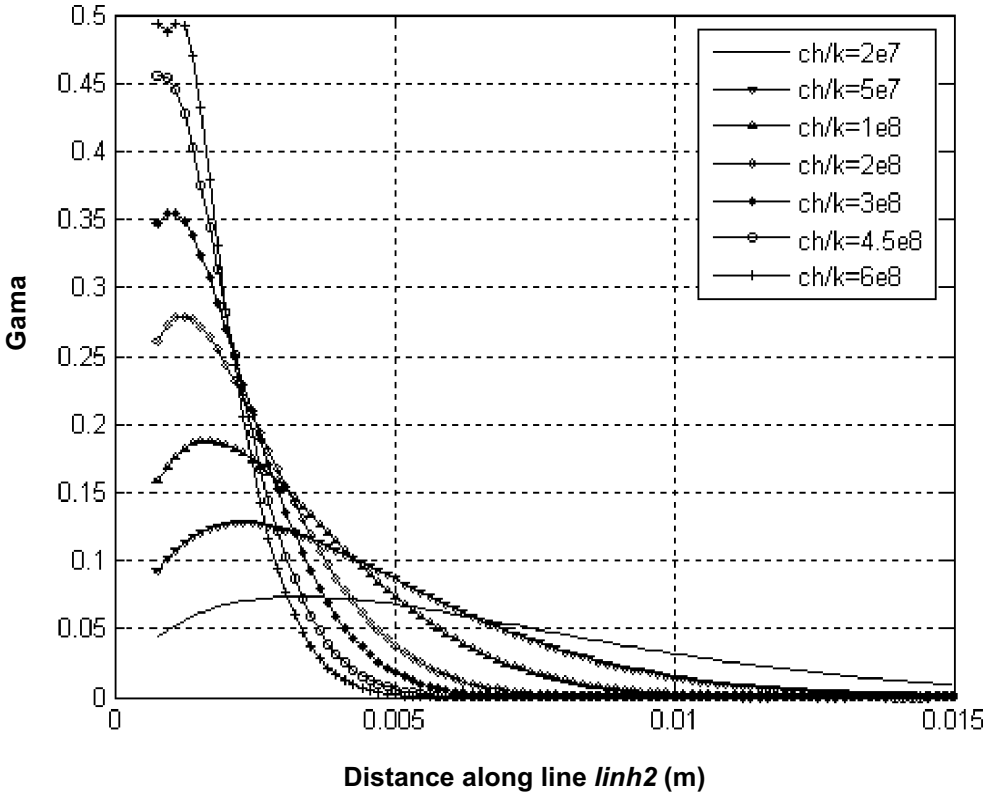

a

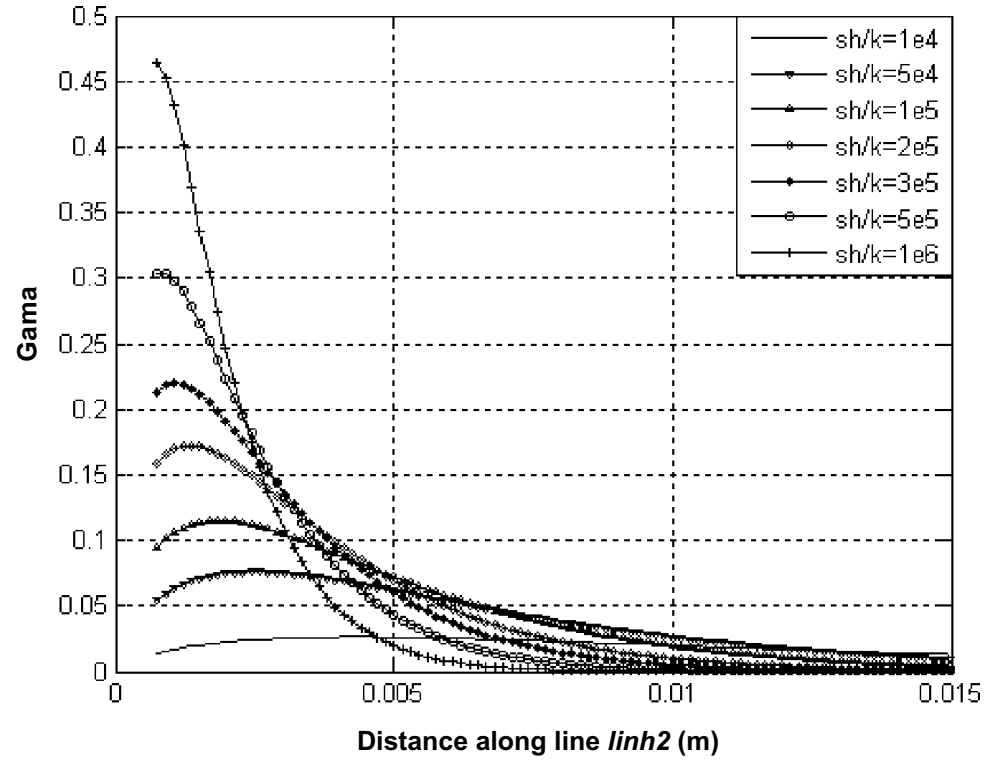

b

Fig. 7. **Volumetric saturation factor values along line *linh2* obtained at:** a – $\frac{S_h}{k} = 0$ and different values of $\frac{C_h}{k}$; b – $\frac{C_h}{k} = 0$ and different values of $\frac{S_h}{k}$.

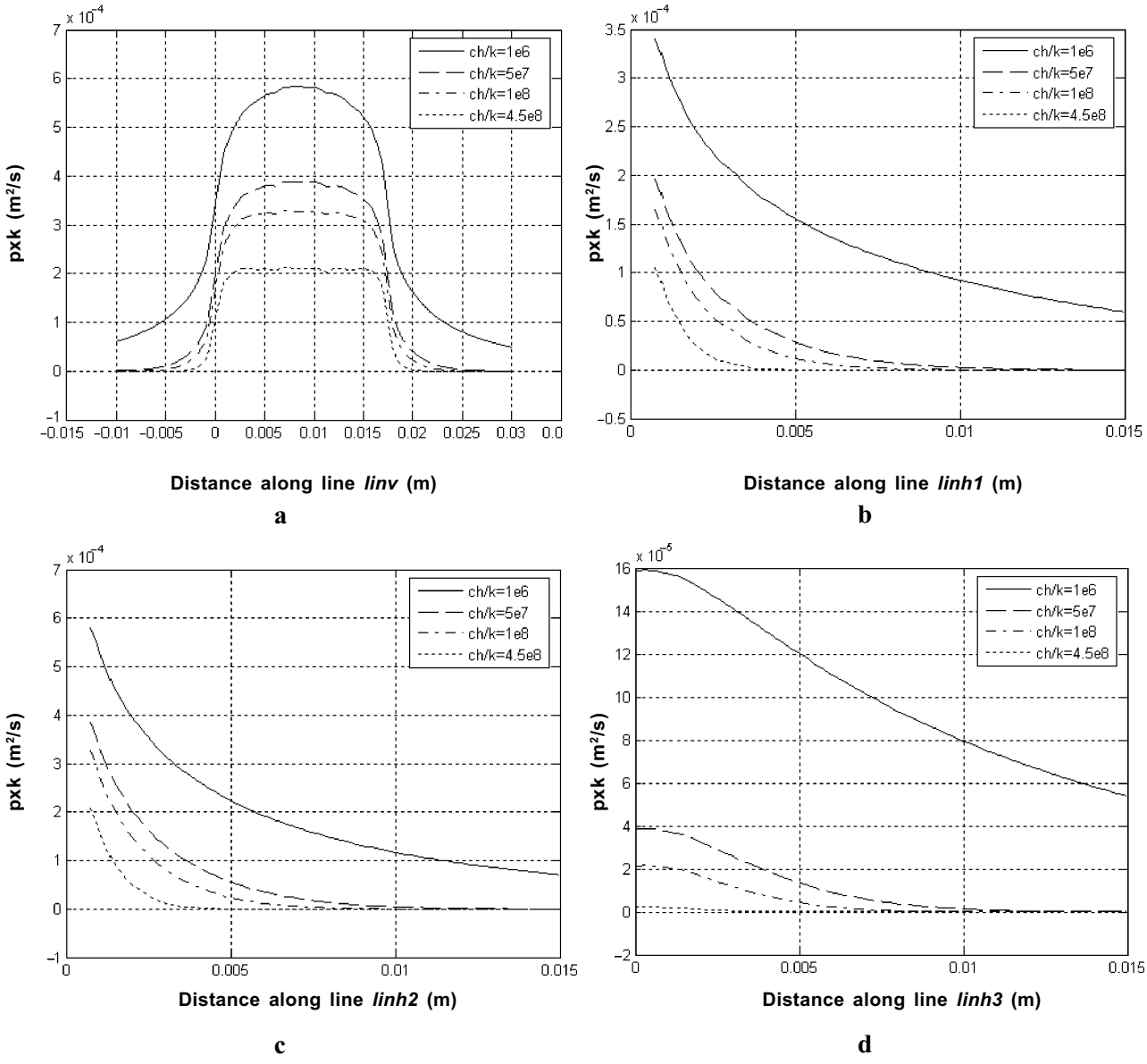

Fig. 8. **Pressure values of injected solution along lines *linv* (a), *linh1* (b), *linh2* (c), *and linh3* (d) obtained at $\frac{S_h}{k} = 0$ and different values of $\frac{C_h}{k}$ after 10 min of injection at a rate of 90 mL/h**

disposed within the tumor tissue, which is a more solid structure, not intersected with tubular structures of significant calibers, thus fluid distribution within the tumor might be different. However, the most clinically important result of RFA is to obtain a zone of total necrosis in liver tissue surrounding the tumor. Thus, the pattern of fluid distribution within the liver tissue seems to be of utmost significance. As it is seen in the experimental images (Fig. 3) compared against computational results (Fig. 6), the obtained shape of the zone saturated with the colored sodium chloride solution in the vicinity of the probe may be distorted as the solution is sewed away through empty blood vessels. The maximum VSF value is still governed by the ratio of the hydraulic capacity to hydraulic conductivity coefficient. Much more detailed and precise experiments would be necessary in order to determine the VSF distribution in the tissues near the ablation probe. Such information enables to find real values of hydraulic capacity and conductivity coefficients and the distribution of "wells" in the model ensuring good conformity with the real physical situation. However, it may be reasonably assumed that even without exact knowledge of real geometry of blood vessels, the principal effects can be approximately modeled. Practically, during experimental injections with

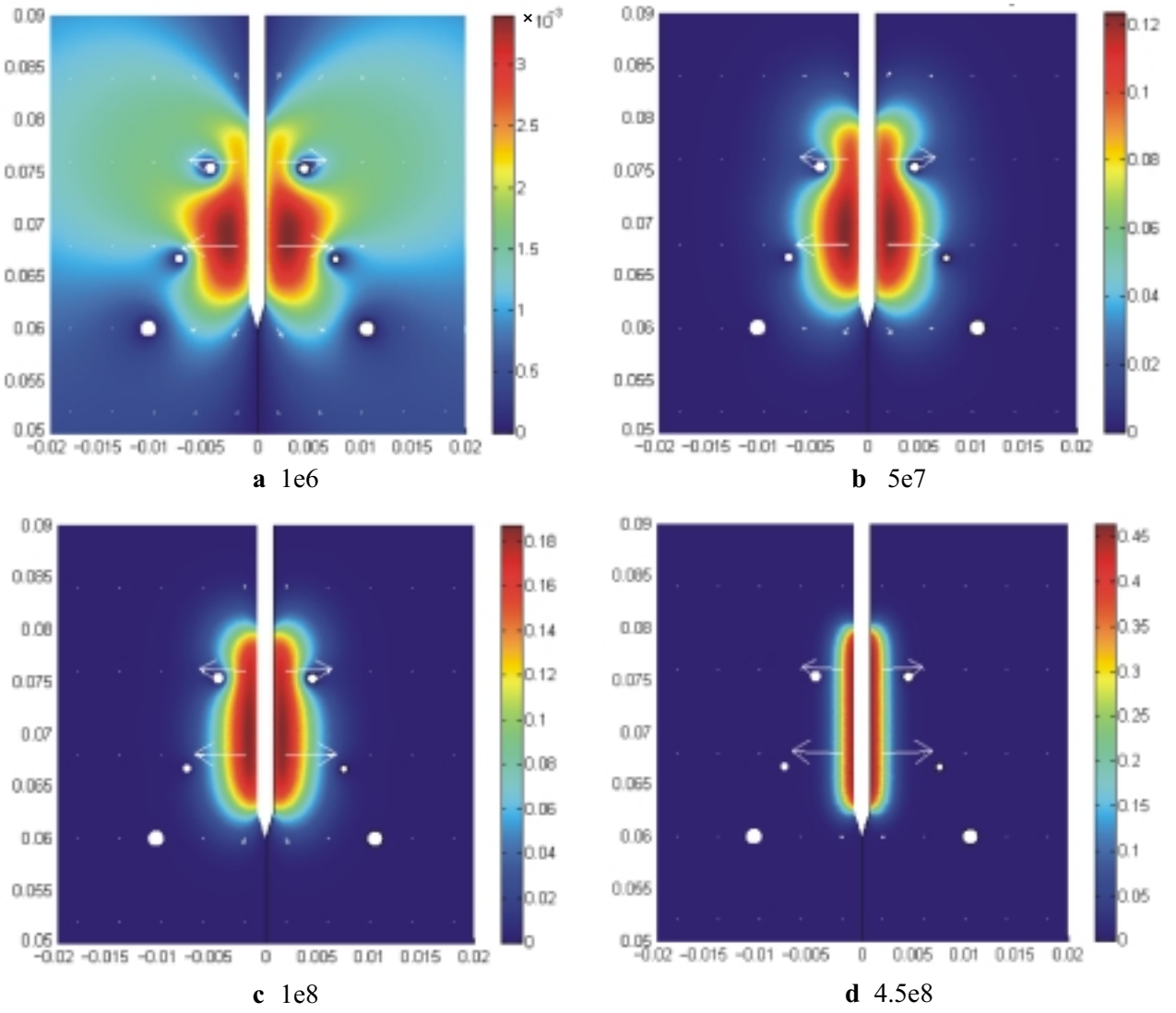

Fig. 9. **Distribution of volumetric saturation factor in the vicinity of the probe if large empty blood vessels are situated in the vicinity of the probe after 10 min injection of sodium chloride solution at a rate of 90 mL/h and $\frac{S_h}{k}$ =0:**

$$a - \frac{c_h}{k} = 10^6; \quad b - \frac{c_h}{k} = 5\times10^7; \quad c - \frac{c_h}{k} = 1\times10^8; \quad d - \frac{c_h}{k} = 4.5\times10^8$$

a non-guided placement of the probe, it is hardly possible to know the true geometry of blood vessel net. Therefore, the characteristics of infiltration velocities and saturation level can always provide only approximate information. Supporting the proposition obtained experimental data show close saturation level results in different liver tissue preparations, while the existing variations may accordingly be attributed to differences in distribution of major vascular structures. The influence of smaller blood vessels can be modeled by the tissue hydraulic capacity mechanism.

The prospective research intends to use the obtained results for the development of complex models of electro-thermal heating coupled with heat advection by means of infiltrated sodium chloride solution.

Conclusion

The Darcy's flow with saturation model can serve only as an approximation of the real infiltration process in the liver tissue.

Idealized models of empty blood vessels in the vicinity of the injection probe have been used, presented as wells able to divert the injected solution far away from the injection zone.

The values of the hydraulic conductivity, capacity, and absorption coefficients of the liver tissue have been determined representing the overall injection and infiltration process. The congruence of the modeling

results against the experiment may be regarded as satisfactory.

The infused solution actively infiltrates liver tissue and might be associated with heat distribution, thus it should be regarded in computational models of radiofrequency ablation.

Acknowledgement

The Lithuanian Science and Studies Foundation sponsored the study.

Natrio chlorido tirpalo infiltracijos į negyvą kepenų audinį matematiniai ir eksperimentiniai tyrinėjimai

Rimantas Barauskas, Antanas Gulbinas[1], Giedrius Barauskas[2]

Kauno technologijos universiteto Sistemų analizės katedra, Kauno medicinos universiteto
[1]Biomedicininių tyrimų institutas, [2]Chirurgijos klinika

Raktažodžiai: radijo dažninė abliacija, matematinis modeliavimas, hidraulinis laidumas, eksperimentiniai tyrimai.

Santrauka. *Tyrimo tikslas.* Sukurti infiltruojamo į kepenų audinį radijo dažninės abliacijos metu skysčio plitimo matematinį modelį.

Metodai. Sukūrėme baigtinių elementų skaičiuojamąjį modelį, imituojantį radijo dažninės abliacijos metu infiltruojamo skysčio plitimą kepenų audinyje, atsižvelgdami į Darcy's greitį, slėgį bei tūrinę audinio įsotinimo frakciją. Modelio lygtyse kepenys traktuojamos kaip porėtoji terpė, pasižyminti tam tikru injekuojamo skysčio hidrauliniu laidumu, talpa bei absorbcijos mechanizmais. Remiantis netiesine tūrinės įsotinimo frakcijos priklausomybe nuo hidraulinio talpumo ir absorbcijos koeficiento, įvertinta negyvo kepenų audinio geba sukaupti tam tikrą skysčio kiekį.

Siekdami įvertinti tam tikrus neatitikimus tarp skaičiuojamųjų ir eksperimentinių duomenų, panaudojome idealizuotą „tuščių kraujagyslių", esančių injekcinės adatos aplinkoje ir galinčių nukreipti tam tikrą skysčio kiekį tolyn nuo destrukcijos zonos, modelį. Šis modelis buvo realizuotas „COMSOL Multiphysics" skaitmeninio modeliavimo terpėje. Atlikome eksperimentinius negyvo kepenų audinio tyrinėjimus, siekdami nustatyti skysčio infiltracijos ypatybes ir apskaičiuoti maksimalų kepenų tūrio padidėjimą injekavus skystį į tam tikro tūrio negyvų kepenų audinio preparatą.

Rezultatai. Lygindami skaičiuojamojo modelio ir eksperimentinius duomenis, nustatėme reikalingas hidraulinio laidumo, talpos bei audinių absorbcijos fizikines konstantas. Gautas patenkinamas skaičiuojamojo modelio ir eksperimentinių duomenų atitikimas.

Išvada. Sukurtas modelis analizuoja injekuojamo skysčio pasiskirstymą kepenų audinyje atsižvelgiant į kepenų audinio hidraulinį laidumą, talpą bei absorbcijos mechanizmus. Gauti duomenys bus taikomi kuriant sudėtingesnius radijo dažninės destrukcijos modelius, kuriais bus įvertinami ir šilumos pernašos procesai, sąlygoti injekuojamo skysčio pasiskirstymo kepenų audinyje.

Adresas susirašinėti: G. Barauskas, KMU Chirurgijos klinika, Eivenių 2, 50009 Kaunas
El. paštas: giedrius.barauskas@gmail.com

References

1. Barauskas R, Gulbinas A, Barauskas G. Investigation of radiofrequency ablation process in liver tissue by finite element modeling and experiment. Medicina (Kaunas) 2007;43(4):310-25.
2. Chang IA, Nguyen UD. Thermal modeling of lesion growth with radiofrequency ablation devices. Biomed Eng Online 2004;3(1):27.
3. Chang I. Finite element analysis of hepatic radiofrequency ablation probes using temperature-dependent electrical conductivity. Biomed Eng Online 2003;2:12.
4. Bear J. Dynamics of fluids in porous media. New York: American Elsevier; 1972.

Received 5 October 2006, accepted 17 April 2007
Straipsnis gautas 2006 10 05, priimtas 2007 04 17